

DOI: <https://doi.org/10.24425/amm.2022.141068>M. SZPUNAR<sup>1\*</sup>, T. TRZEPIECIŃSKI<sup>1,2</sup>, R. OSTROWSKI<sup>3</sup>, M. ZWOLAK<sup>3</sup>

## RESEARCH ON FORMING PARAMETERS OPTIMIZATION OF INCREMENTAL SHEET FORMING PROCESS FOR COMMERCIAL PURE TITANIUM GRADE 2 SHEETS

This study aims to determine optimal forming parameters for Incremental Sheet Forming process Commercially Pure titanium Grade 2 sheets in terms of formability improvement, force reduction, and efficiency of forming. Based on the central composite design, data were collected during 20 runs and then variation analysis was performed. The experiments were performed on a 3 axis CNC milling machine equipped with a Kistler dynamometer plate. Subsequently, regression models have been developed to describe process responses by input factors. As crucial parameters, the relative velocity and step size of the tool that affect the forming force and the height of the fracture have been determined. Finally, the application of optimization algorithm has emerged optimal input factors in terms of selected multi-criteria goal. The results of this study suggest that there is a process window that allows the formation of 45° wall angle drawpieces of commercially pure titanium Grade 2.

*Keywords:* incremental sheet forming; forces; fracture; parameter optimization; titanium

### 1. Introduction

The area of incremental sheet-forming processes (ISF) is attracting increasing attention due to its flexibility, low implementation cost, and less problematic than conventional stamping, within a wide range of applications [1]. The process takes advantage in custom parts, small batches, as well as prototypes, which can be easily adopted in aerospace [2,3], automotive [4,5] and medical industries [6,7]. Incremental forming does not require a dedicated die and tool; generally, a set of equipment allows one to form different types of materials and part shapes. By ISF, a higher value of deformation is possible, as well as lower forces required to realize the process [8]. Moreover, the formation limit curve is more beneficial in comparison to conventional forming [9,10].

Titanium Grades have wide range of application in many sectors due to high strength to weight ratio along with high strength at elevated temperatures, excellent corrosion resistance, biocompatibility and weldability. The ISF technique has a potential in titanium formation, however, depending on the titanium grade, in some cases an additional heat source is demanded to improve deformation, shape accuracy and reduce springback effect [11]. One of the possibilities of raising the

sheet temperature is by friction between the tool and the work-piece. An increase in tool rotation speed leads to heat generation, although excessive temperature in combination with tool rotation may advance to galling and sheet perforation. Otsu [12] investigated the influence of the relative tool rotational speed at a constant feedrate. In his work, a 35° angle truncated cone made of commercially pure titanium with a thickness of 0.4 mm were formed. The author determined process window allowing to obtain 20 mm height drawpieces, however, could not achieve slope angle 45°. Kumar and Tandon [13] found that elevated temperature reduces the forming force by up to 30% for Ti-Grade 2 relative to room temperature. The lower forming force may suggest reduction of the springback effect, as well as decrease in shape deviation [11]. Several optimizations of the ISF process have already been conducted. Majagi and Chandramohan [14] carried out a Box-Behnken design of an experiment with Response Surface Methodology by varying feedrate, tool RPM, and coolant flow rate to analyze surface roughness, thickness reduction, as well as hardness and grain size after forming the AA6061 sheet. The authors found optimal feedrate 50.74 mm/min, tool RPM 300.74 1/min and coolant flow 3.27 l/min for selected criteria in range of the experiment. Gulati et al. [15] selected the Taguchi method to optimize the wall

<sup>1</sup> RZESZOW UNIVERSITY OF TECHNOLOGY, DOCTORAL SCHOOL OF ENGINEERING AND TECHNICAL SCIENCES, 8 POWST. WARSZAWY AV., 35-959, RZESZÓW, POLAND

<sup>2</sup> RZESZOW UNIVERSITY OF TECHNOLOGY, DEPARTMENT OF MANUFACTURING AND PRODUCTION ENGINEERING, 12 POWST. WARSZAWY AV., 35-959, RZESZÓW, POLAND

<sup>3</sup> RZESZOW UNIVERSITY OF TECHNOLOGY, DEPARTMENT OF MATERIALS FORMING AND PROCESSING, 12 POWST. WARSZAWY AV., 35-959, RZESZÓW, POLAND

\* Corresponding author: [d547@stud.prz.edu.pl](mailto:d547@stud.prz.edu.pl)



angle and surface roughness. The authors found that lubrication plays an important role in surface quality and sheet formability. Hrairi et al. [16] performed Gray-Taguchi ISF optimization that resulted in an improvement of 27.4% process from the mean grade value. Kumar and Elangovan [17] obtained a satisfactory optimization agreement with the experiment for Inconel 718 ISF by adopting a central composite design with surface response methodology. The authors found feedrate 3000 mm/min, step size 0.2 mm and lubrication viscosity 105.606 mm<sup>2</sup>/s to be the most favourable in case of optimization criteria with 98% accuracy to model prediction. However, there is a gap in the literature on the proper selection of ISF parameters for commercially pure titanium grades to minimize the forces and eliminate the crack, achieving an improvement in the height of the drawpiece. This study aimed to establish multi-criterial optimal process input parameters with the statistical method. The experiment was based on a central composite design with analysis of variance that led to the development of the regression model and finally the optimization algorithm.

TABLE 1

Mechanical Properties of Titanium Grade 2 [18]

Density	4.51 g/cm <sup>3</sup>
Tensile Strength, Ultimate	430 MPa
Tensile Strength, Yield	340 MPa
Elastic modulus	102 GPa
Hardness	235 HV

## 2. Materials and methods

As a test material, Grade 2 commercially pure Titanium sheets in annealed condition were chosen with a thickness of 0,4 mm. TABLE 1 presents the mechanical properties of the material selected for the incremental formation of samples.

The experiments were carried out with the use of a 3-axis CNC milling machine Makino PS95. A special fixture designed for the incremental sheet formation process was located on a Kistler piezoelectric dynamometer plate inside the machine working zone. As a forming tool, a hemispherical ended tungsten carbide rod  $\varnothing 8$  mm grade ISO K30-K40 was applied and mounted in an ER32 collet chuck. The sheet specimens were cut into a circular shape  $\varnothing 100$  mm and clamped with a 10 screws tightened to a torque of 10 Nm. To decrease friction between the tool and the workpiece, 75W-85 oil lubricant has been deposited. The role of Kistler dynamometer plate was to measure forming forces while CNC axis display to read out fracture depth position. Fig. 1 presents the test stand for the incremental formation process. A truncated cone geometry with wall angle 45° has been determined as a drawpiece shape (Fig. 2). Through the NX Siemens CAD/CAM software application, a spiral tool path has been created for the CNC machine. The step size parameter determines the increment in the drawpiece height per one circular tool pass. Fig. 3 presents one of the specimens shaped from the experiment where no breakage occurs.

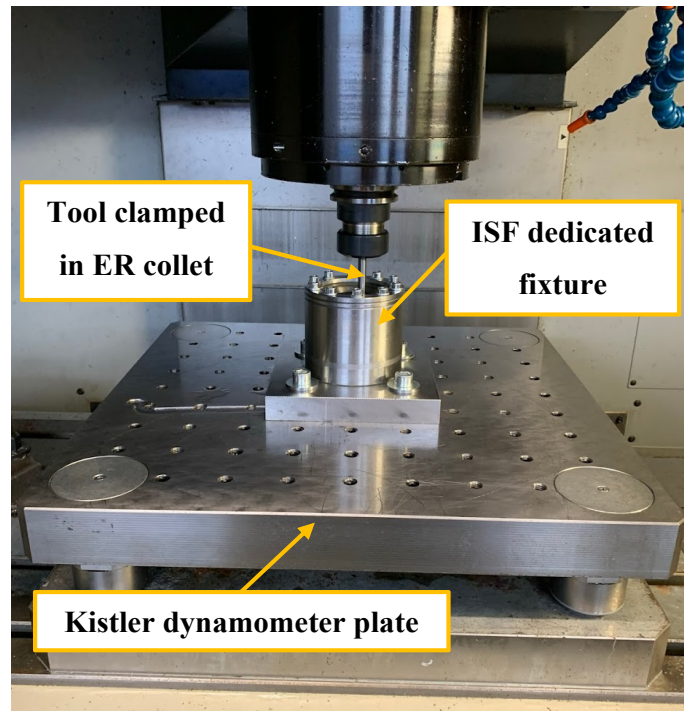


Fig. 1. Test stand for the ISF process

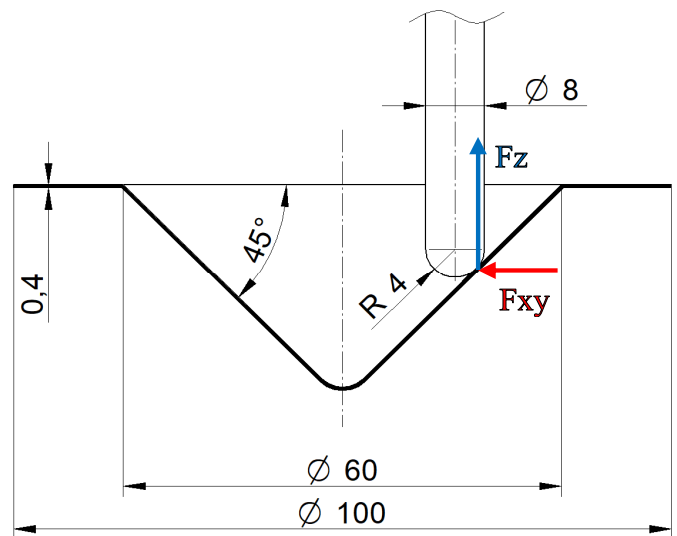


Fig. 2. Specimen geometry and forming force distribution



Fig. 3. One of the successfully obtained drawpieces

TABLE 2

Summary and coding of input factors

Factor	Name	Units	Type	Min	Max	Coded Low	Coded High	Mean	Std. Dev.
A	Tool RPM ( <i>n</i> )	1/min	Numeric	-789.64	789.64	-1 ↔ -600	+1 ↔ 600	52.50	495.05
B	Feedrate ( <i>V<sub>f</sub></i> )	mm/min	Numeric	262.94	2237.06	-1 ↔ 500	+1 ↔ 2000	1250	582.58
C	Step size	mm	Numeric	0.0368	0.5632	-1 ↔ 0.10	+1 ↔ 0.50	0.30	0.1554

The purpose of the investigation was to obtain optimal forming parameters with respect to maximizing forming efficiency and minimizing forming forces, achieving a crack-free part to its full depth (28.3 mm). To realize this challenging task, a central composite design statistic method has been performed. Data analysis was performed with Design-Expert 12 software. As input parameters, tool RPM, feedrate and step size have been determined by a range of established in literature and correlation with initial tries. Then the input factors have been extended by

the practical alpha value – the fourth root of the number of input factors, which equals 1.316. Input parameter design presents TABLE 2.

Fig. 4 shows 20 runs of the experiment distributed in a cubic design space. Regression analysis with ANOVA support was used to predict the output. The resulting forming force parameter *F<sub>max</sub>* is a maximum acquisition of the 3-axis forces component (*F<sub>z</sub>* – axial, *F<sub>xy</sub>* – radial) DAQ that existed during the specified run in the formation period of time. Fig. 5 presents an example force plot with methodology for *F<sub>max</sub>* reading. The tool RPM has been converted to a linear velocity at the maximum contact diameter *V<sub>c</sub>* using the equation. (1) and compensated by the corresponding feedrate speed *V<sub>f</sub>* using Eq. (2). Fig.6 presents velocity vectors. Minus sign before the tool RPM means that the tool rotates in a clockwise direction, while the positive value indicates that the tool rotation is counter clockwise. As a consequence of conversion tool, contact velocity has been coded 1 as low and 15 as high.

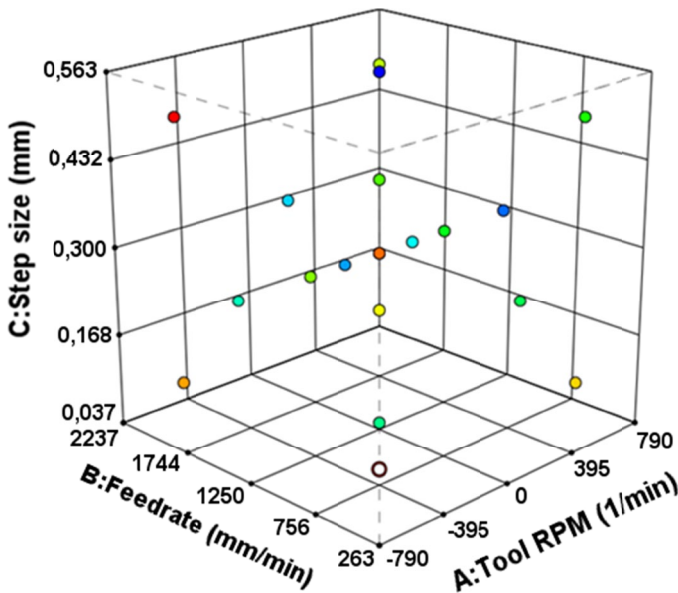


Fig. 4. Set of designed runs

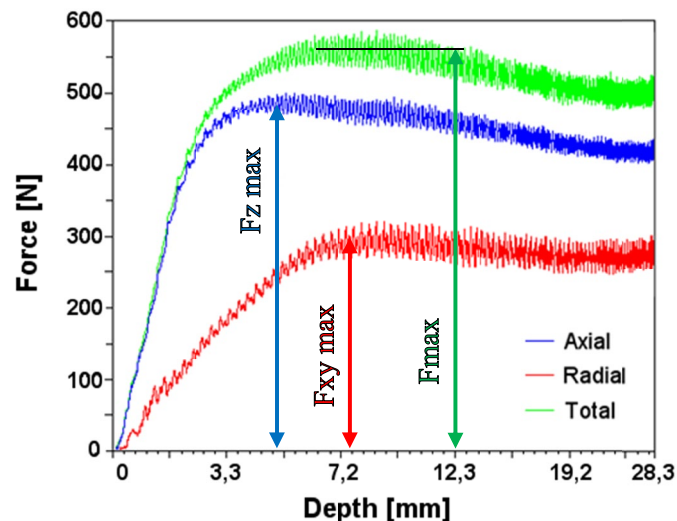


Fig. 5. Component force plot with reference to time

### 3. Results and discussion

The data obtained from the experiment with input factors and response values are presented in TABLE 3. ANOVA and regression analysis are performed for each response separately. At the beginning, model degree selection is determined by comparison of several indicators: Model p-value, lack of fit p-value, adjusted *R<sup>2</sup>* and predicted *R<sup>2</sup>*. The first two inform about statistical significance – a lower p-value means a higher significance. The *R<sup>2</sup>* parameters describe how the experiment data fit to the model, values close to 1 are demanded, and nearly 0 should be completely rejected. TABLE 4 presents the fit summary for the model selection for total force response output.

Subsequently, the backward elimination algorithm is applied. It eliminates model sources whose p-values are higher than 0.1 – this means that the factor is statically insignificant and should be rejected. This treatment improves the precision of the model. However, if the lower degree factor is insignificant, although the higher level is, the hierarchical rule is preserved and both factors remain in the model. The same procedure of analysis has been performed for the forming height response.

$$V_c = \frac{\pi \times 5.66 \times n}{1000} \quad (1)$$

$$V_r = |V_c - V_f| \quad (2)$$

TABLE 3

Experiment results with respect to input factors

Run	Factor 1 A: Tool contact velocity ( $V_r$ ) m/min	Factor 2 B: Feedrate ( $V_f$ ) m/min	Factor 3 C: Step size mm	Response 1 Resultant force N	Response 2 Fracture height mm
1	1.25	1.25	0.56	863	7.6
2	1.25	1.25	0.30	697	6.6
3	12.80	1.25	0.30	562	28.3
4	4.81	1.25	0.30	712	28.3
5	1.32	2.24	0.30	652	7.9
6	2.31	1.25	0.30	625	6.8
7	15.30	1.25	0.30	543	28.3
8	1.25	1.25	0.04	452	5.5
9	0.26	0.26	0.30	674	5.6
10	5.86	1.25	0.30	628	28.3
11	10.17	0.50	0.50	598	28.3
12	11.17	0.50	0.50	599	28.3
13	8.36	1.25	0.30	632	28.3
14	8.67	2.00	0.50	681	28.3
15	8.67	2.00	0.10	465	28.3
16	10.17	0.50	0.10	419	28.3
17	12.67	2.00	0.10	479	28.3
18	1.25	1.25	0.30	666	5.9
19	11.17	0.50	0.10	401	28.3
20	10.87	2.00	0.50	663	28.3

TABLE 4

Summary of the fit for the the variety models for resultant force response

Source	Model p-value	Lack of Fit p-value	Adjusted $R^2$	Predicted $R^2$	
Design Model	<0.0001	0.4118	0.8867	0.5785	
<b>Linear</b>	<b>&lt;0.0001</b>	<b>0.3583</b>	<b>0.8450</b>	<b>0.7941</b>	<b>Suggested</b>
2FI	0.0718	0.4101	0.8866	0.8592	
<b>Quadratic</b>	<b>0.0387</b>	<b>0.5148</b>	<b>0.9339</b>	<b>0.6303</b>	<b>Suggested</b>
Cubic	0.9224	0.3520	0.8830		Aliased

**Resultant force**

As the summary of model fit (TABLE 4) shows, the linear and quadratic models are recommended. Both models were investigated to the ANOVA analysis and the backward elimination procedure. However, the reduced quadratic model turned out to be a better fit with the result  $R^2 = 0.9652$ , Adjusted  $R^2 = 0.9449$ , Predicted  $R^2 = 0.8281$  compared to  $R^2 = 0.8497$ , Adjusted  $R^2 = 0.8320$ , Predicted  $R^2 = 0.7823$  for the reduced linear one respectively. Bearing this collation in mind, the reduced quadratic model was finally selected. TABLE 5 presents the ANOVA results for a reduced quadratic model that describes the resultant force output. The whole input factors are significant. The resulting force model in terms of coded input

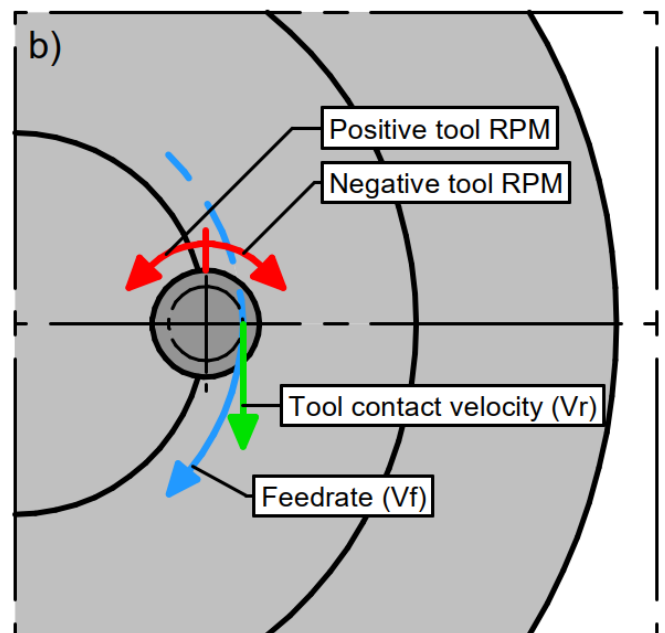
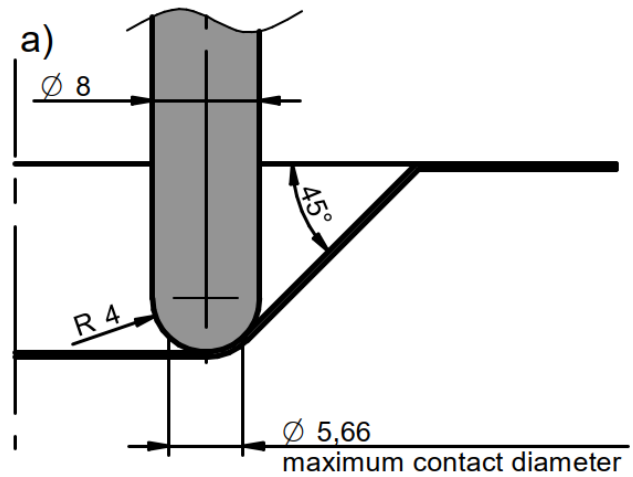


Fig. 6. Method for tool speed calculation; a) for wall angle 45° and hemispherical tool diameter Ø8 mm; b) Tool contact velocity relative to tool RPM direction and feedrate

factors is shown in Eq. (3). The A factors lead to a decrease in the formation forces. This effect can be explained by an elevated temperature that improves deformation as a consequence of friction between the tool and the workpiece. The high level of step size (C-factor) seems to be the main reason for the elevated forces. The effect of input on the resultant force has been presented using response surfaces. (Fig. 7) The Model F-value of 47.56 suggests that the model is significant. There is only a 0.01 % chance that the noise caused such a huge F-value. The predicted  $R^2 = 0.828$  is compatible with the adjusted  $R^2 = 0.945$ , the discrepancy is less than 0.2.

$$\begin{aligned}
 \text{Resultant force} = & 617.474 - 75.4838A + \\
 & + 21.4868B + 111.669C + 26.4886AB + \\
 & - 45.9165AC - 25.4224B^2 - 24.2186C^2 \quad (3)
 \end{aligned}$$

TABLE 5

ANOVA table for the resultant force model

Source	Sum of Squares	df	Mean Square	F-value	p-value	
Model	2.398E+05	7	34257.28	47.56	<0.0001	significant
A-Tool contact velocity	50625.59	1	50625.59	70.28	<0.0001	
B-Feedrate	5225.61	1	5225.61	7.25	0.0195	
C-Step size	1.418E+05	1	1.418E+05	196.79	<0.0001	
AB	3380.66	1	3380.66	4.69	0.0511	
AC	9244.21	1	9244.21	12.83	0.0038	
B <sup>2</sup>	4584.22	1	4584.22	6.36	0.0268	
C <sup>2</sup>	4131.62	1	4131.62	5.74	0.0338	
Residual	8643.97	12	720.33			
Lack of Fit	8163.47	11	742.13	1.54	0.5619	not significant
Pure Error	480.50	1	480.50			
Cor Total	2.484E+05	19				
Std. Dev.	26.84			<i>R</i> <sup>2</sup>	0.9652	
Mean	600.55			Adjusted <i>R</i> <sup>2</sup>	0.9449	
C.V. %	4.47			Predicted <i>R</i> <sup>2</sup>	0.8281	
				Adeq Precision	26.1716	

Factor Coding: Actual

Resultant force (N)

401  863

X1 = A

X2 = B

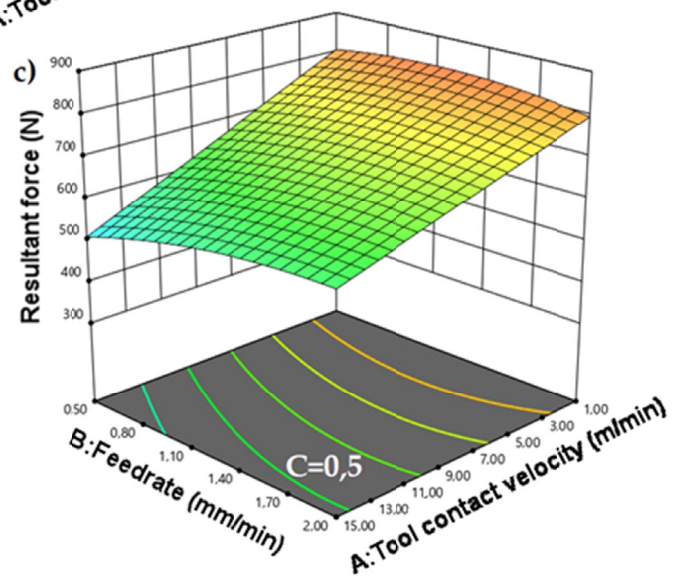
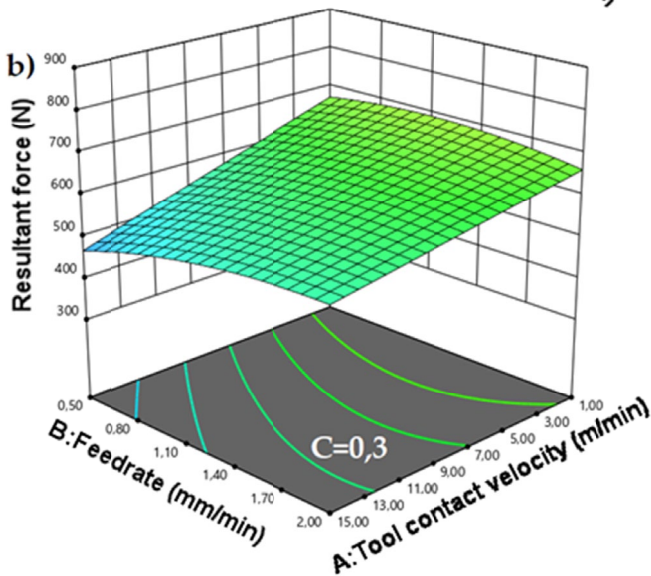
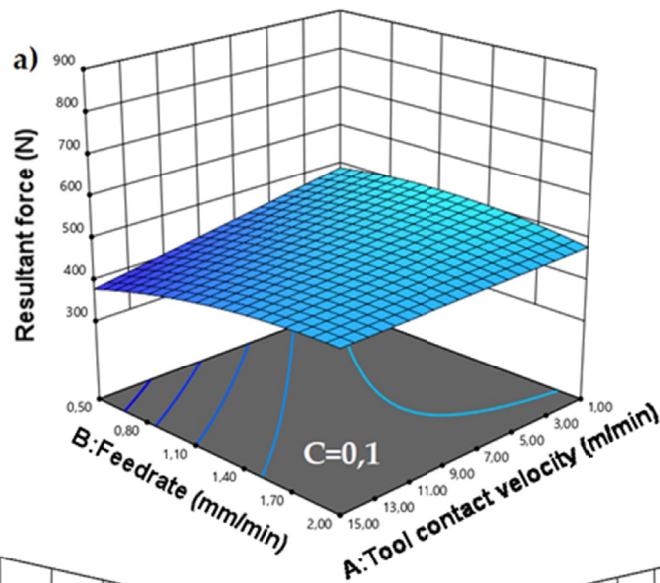


Fig. 7. Response surfaces for the resultant force in case of different step size values; a) low  $C = 0.1$ ; b) medium  $C = 0.3$ ; c) high  $C = 0.5$

ANOVA table for the resultant fracture height model

Source	Sum of Squares	df	Mean Square	F-value	p-value	
Model	2015.51	2	1007.75	121.56	<0.0001	significant
A-Tool contact velocity	614.05	1	614.05	74.07	<0.0001	
A <sup>2</sup>	332.47	1	332.47	40.11	<0.0001	
Residual	140.93	17	8.29			
Lack of Fit	140.68	16	8.79	35.89	0.1305	not significant
Pure Error	0.2450	1	0.2450			
Cor Total	2156.44	19				
Std. Dev.	2.88			R <sup>2</sup>	0.9346	
Mean	20.69			Adjusted R <sup>2</sup>	0.9270	
C.V. %	13.92			Predicted R <sup>2</sup>	0.8887	
				Adeq Precision	24.2866	

### Fracture height

TABLE 6 presents ANOVA results for a reduced quadratic model that describes the drawpiece breakage height. Equation 4 shows the fracture height model in terms of coded input factors. The model consists of tool contact velocity factor alone. The rest factors were reduced by backward elimination because of their insignificance. The effect of the input source  $A$  and  $A^2$  on the height of the fracture has been presented in a one-factor plot (Fig. 8). Tool contact velocity effects on amount of heat generated by a friction between tool and workpiece. However, excessive velocity may cause overheating leading to failure. The Model F-value of 121.56 suggests that the model is significant. There is only a 0.01 % chance that the noise caused such a huge F-value. The predicted  $R^2 = 0.888$  is compatible with the adjusted  $R^2 = 0.927$ , the discrepancy is less than 0.2.

$$\text{Fracture height} = 27.7519 + 9.70055A - 11.7539A^2 \quad (4)$$

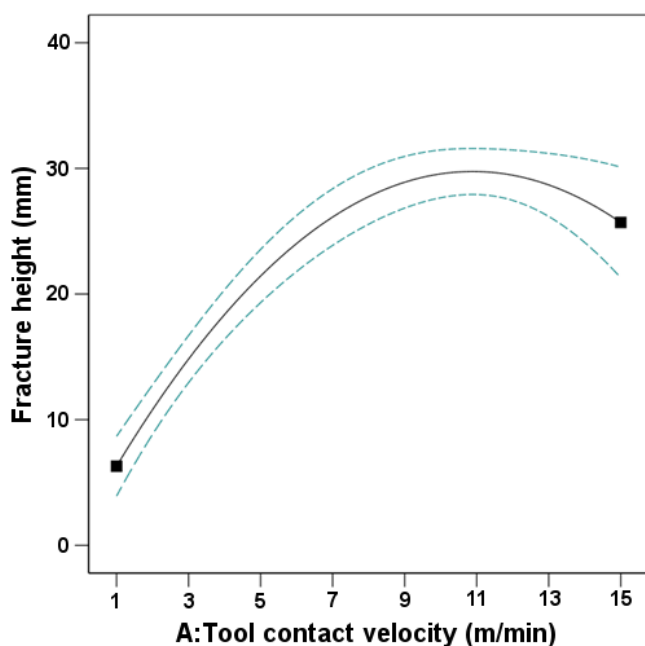


Fig. 8. One-factor graph for fracture height relative to tool contact velocity

### Optimization

To solve the parameter selection problem of the process, a hill climbing algorithm has been implemented for the created models. The goal of optimization was to obtain fully-heighted drawpiece – 28.3 mm height without any fracture while keeping lowest resultant forming forces with maximum forming performance. For each factor and the response importance parameter, a higher value means that the criterion is more desirable and the development goal will be more focused on achieving this parameter improved than others.

TABLE 7 presents constraints for the optimization algorithm solutions obtained in response to the selection criteria. The bar graph in Fig. 9 shows desirability indicators; it informs how successful the target of a given parameter has been reached (1 means that the optimization meets the requirements completely, 0 none). 23 solutions have been found for selected goals, however, one with highest combined desirability has been chosen. Fig. 10 presents the solution with the highest desirability for the selected constraints.

TABLE 7

Optimization criteria for input and output process parameters

Name	Goal	Lower Limit	Upper Limit	Importance
A: Tool contact velocity	is in range	1	15	—
B: Feedrate	maximize	0.5	2	1
C: Step size	maximize	0.1	0.5	1
Resultant force	minimize	401	863	2
Fracture height	maximize	5.5	28.3	3

### 4. Conclusions

This paper has shown optimal parameter selection with a statistical method experiment for incremental forming of CP titanium grade 2. The data presented here underlie the process

window to achieve 45° wall angle drawpieces. Results allow to form the following conclusions:

- In case of maximum forming force value, tool relative velocity and feedrate are significant, while step size is the most influential. Forces can be reduced by increasing tool relative velocity, while step size remains high.
- A key role in drawpiece height plays a tool relative velocity, its proper selection decide about forming success.
- Obtained parameter adequate precision for models: forming force and fracture height 26.1716 and 24.2866 respectively, allows to navigate in the design space.
- Optimal input factors for selected criteria are tool contact velocity 13.35 m/min, feedrate 2 m/min and step size 0.5 mm.

The present findings might help to solve the problem of proper parameter selection which may lead to a higher angle of deformation in the perspective. Future research should consider the potential effects of process parameters on sheet thinning as well as springback analysis and drawpiece shape accuracy.

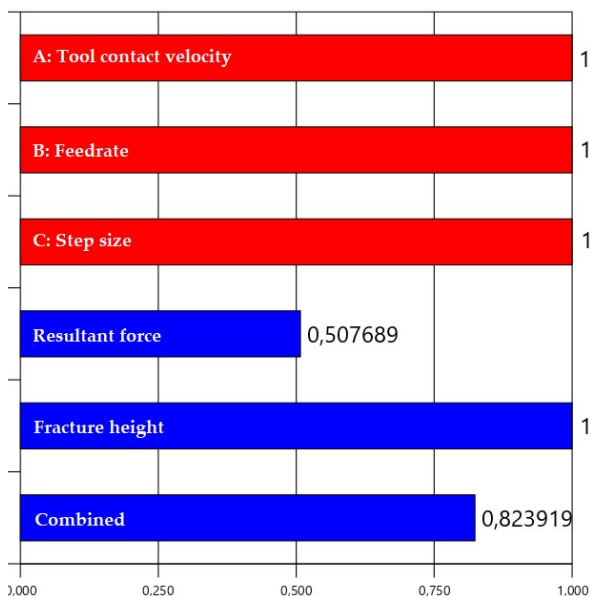


Fig. 9. Desirability results for each parameter in case of optimization target

## REFERENCES

- [1] T. Trzepieciński, H.G. Lemu, *Metals* **10**, 47 (2020). DOI: <https://doi.org/10.3390/met10010047>
- [2] T. Trzepieciński, B. Krasowski, A. Kubit, D. Wydrzyński, *Mechanika* **298**, 87-100 (2018). DOI: <https://doi.org/10.7862/rm.2018.08>
- [3] T. Trzepieciński, V. Oleksik, T. Pepelnjak, S.M. Najm, I. Paniti, K. Maji, *Metals* **11**, 1188 (2018). DOI: <https://doi.org/10.3390/met11081188>
- [4] I. Peter, E. Fracchia, I. Canale, R. Maiorano, *Procedia Manufacturing* **32**, 50-58 (2019). DOI: <https://doi.org/10.1016/j.promfg.2019.02.182>
- [5] S. Scheffler, A. Pierer, P. Scholz, S. Melzer, D. Weise, Z. Rambousek, *Procedia Manufacturing* **29**, 105-111 (2019). DOI: <https://doi.org/10.1016/j.promfg.2019.02.112>
- [6] Z. Cheng, Y. Li, C. Xu, Y. Liu, S. Ghafoor, F. Li, *J. Mater. Res.* **9**, 7225-7251 (2020). DOI: <https://doi.org/10.1016/j.jmrt.2020.04.096>
- [7] P.K. Bhojar, A.B. Borade, *Biomed. Eng.* **31**, 352-357 (2015). DOI: <https://doi.org/10.1590/2446-4740.0705>
- [8] A. Kumar, V. Gulati, P. Kumar, H. Singh, *J. Braz. Soc. Mech. Sci.* **41**, 251 (2019). DOI: <https://doi.org/10.1007/s40430-019-1755-2>

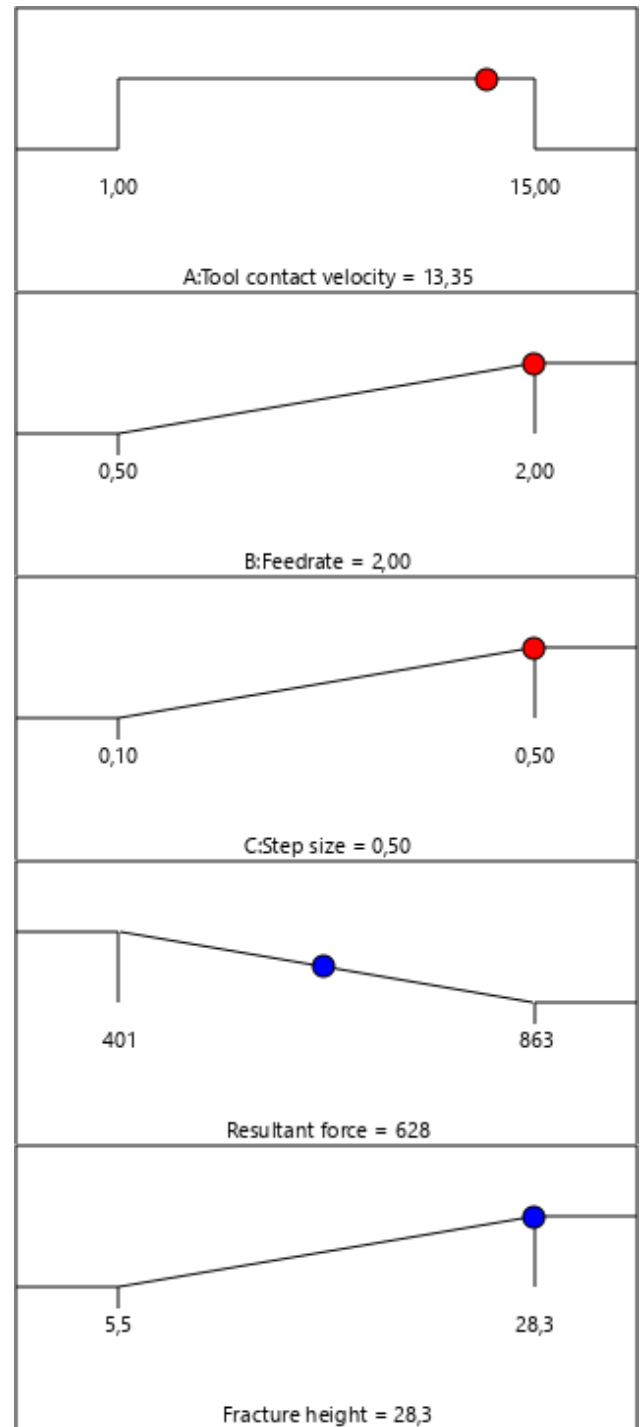


Fig. 10. Ramp graph of the optimal solution

- [9] Y. Kumar, S. Kumar, Incremental Sheet Forming (ISF), Springer, 29-46 (2015). DOI: [https://doi.org/10.1007/978-81-322-2355-9\\_2](https://doi.org/10.1007/978-81-322-2355-9_2)
- [10] S. Gatea, D. Xu, H. Ou, G. McCartney, Int. J. Adv. Manuf. Tech. **95**, 625-641 (2018). DOI: <https://doi.org/10.1007/s00170-017-1195-z>
- [11] V. Oleksik, T. Trzepieciński, M. Szpunar, Ł. Chodoła, D. Ficek, I. Szczęsny, Materials **14**, 6372 (2021). DOI: <https://doi.org/10.3390/ma14216372>
- [12] M. Otsu, Key Eng. Mater. **716**, 3-10 (2016). doi:10.4028/www.scientific.net/KEM.716.3
- [13] P. Kumar, P. Tandon, P. I. Mech. Eng. **235**, 1779-1789 (2021). DOI: <https://doi.org/10.1177/0954405421995669>
- [14] D. Majagi, G. Chandramohan, Appl. Mech. Mater. **527**, 111-116 (2014). DOI: <https://doi.org/10.4028/www.scientific.net/AMM.527.111>
- [15] V. Gulati, A. Aryal, P. Katyal, A. Goswami, J. Inst. Eng. India Ser. C **97**, 185-193 (2016). DOI: <https://doi.org/10.1007/s40032-015-0203-z>
- [16] M. Hrairi, J. I. Daoud, F. Zakaria, IJRTE **7**, 246-252 (2019).
- [17] S.P. Kumar, S. Elangovan, T. Can. Soc. Mech. Eng. **44**, 148-160 (2019). DOI: <https://doi.org/10.1139/tcsme-2019-0003>
- [18] <https://asm.matweb.com/search/SpecificMaterial.asp?bassnum=MTU021>, accessed: 25.03.2022.